# Modeling Dissimilar Optical Fiber Splices With Substantial Diffusion

Jian Luo

***Abstract*—Optical losses of dissimilar fiber fusion splices are modeled using a combination of diffusion simulation and beam propagation method; open-source codes are provided. It is demonstrated that an optimal amount of diffusion is required to achieve the minimum splice loss. Additional annealing beyond the optimal level is detrimental. Furthermore, oscillation of splice loss with the geometrical parameters of the heat zone due to an optical interference effect is revealed, which can be intentionally utilized to reduce dissimilar fiber splice losses. Understanding these diffusion-related splice loss mechanisms is important for splicing process optimization, as well as design of fusion splicers and novel postsplicing heat treatment devices.**

***Index Terms*—Beam propagation method (BPM), diffusion equation, dissimilar fiber splices, optical fibers, splice loss.**

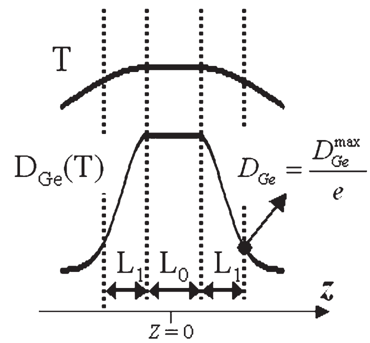


Fig. 1. Representative generic temperature profile of a heat source. $L_0$ and $L_1$ are the widths of constant and transition temperature regions, respectively. The associated diffusivity profile is also shown.

## I. Introduction

WITH THE increasing use of different types of optical fibers, it has become critically important to reduce high dissimilar fiber splice losses that resulted from a mode-field mismatch, which can be greater than 1 dB in some cases [1]. Reducing dissimilar fiber splice losses is particularly challenging if a dispersion-compensated fiber (DCF), an Er-doped fiber (EDF), or a microstructured fiber is involved [2]. High splice losses between dissimilar fibers can be reduced by diffusion-based techniques involving long fusion time [3]–[8] pre and post heat treatments [1]. To date, such splicing process optimization is largely conducted by empirical methods (either trials and errors or design of experiments) [3]–[9].

Various methods have been developed to estimate or compute the optical loss of splices between dissimilar fibers [2], [10], [11], but these methods do not consider the effects of diffusion. Diffusion in thermally expanded core fibers and its impact on splice losses have been analyzed [12], but this approach assumes step-index single-mode fibers and adiabatic model conversion in the diffusion region. On the other hand, the beam propagation method (BPM) has been widely used to characterize optical components. An earlier attempt was made to model splice loss with an overly simplified 2-D model (instead of waveguides with circular symmetry) with limited success [13].

There are distinct benefits to developing and testing rigorous, yet easy-to-implement, methods to model optical characteristics of diffused splices. Such schemes should combine 3-D material diffusion and BPM simulations and treat arbitrary refractive index profiles (RIPs) and less-gradual diffusion zones (nonadiabatic modal conversion). More importantly, this paper is motivated by a critical need to understand the basic underlying loss mechanisms involving diffused dissimilar fibers with a goal of enabling the knowledge-based optimization/design of fusion splicing and heat treatment processes/equipment.

Manuscript received April 28, 2007; revised August 12, 2007.

The author is with the School of Materials Science and Engineering and Center for Optical Materials Science and Engineering Technologies, Clemson University, Clemson, SC 29634-5124 USA (e-mail: jluo@alum.mit.edu; jianluo@clemson.edu).

Digital Object Identifier 10.1109/JLT.2007.907788

## II. Numerical Scheme and Validation

The temperature profile of a fusion (or heat treatment) zone is given by the following generic form:

$$\begin{cases} T = T_{\max}, & \text{if } |z| < \frac{L_0}{2} \\ \frac{Q}{RT} - \frac{Q}{RT_{\max}} = \frac{\left(|z| - \left|\frac{L_0}{2}\right|\right)^2}{L_1^2}, & \text{if } |z| > \frac{L_0}{2} \end{cases}. \tag{1}$$

The geometrical profile of the heat zone is characterized by two parameters, namely $L_0$ and $L_1$, which are the widths of the constant and transition temperature zones, respectively. $Q$ and $R$ are the diffusion activation energy and the gas constant, respectively. Since diffusivity $D = D_0 \exp(Q/RT)$, the outer boundary of the transition temperature zone $(L_1)$ is defined by the condition that the diffusion coefficient is equal to $1/e$ of the maximum value. A representative temperature distribution is shown in Fig. 1.

While the proposed scheme can be applied for arbitrary RIPs, fusion splices between two step-index single-mode fibers are modeled as a numerical example to reveal some basic and universal loss mechanisms. In this specific example, Fiber 1 has a core diameter of 6.0 $\mu$m with a $\Delta n$ of 0.008. Fiber 2 has a core diameter of 4.0 $\mu$m with a $\Delta n$ of 0.020. These are single-mode fibers with mode-field diameters of 8.31 and 5.25 $\mu$m, respectively, at 1550 nm. For simplicity, these fibers are assumed to be Ge doped only. The diffusion equation along the $r$-axis is given by

$$\frac{\partial c_{\mathrm{Ge}}(r,t)}{\partial t} = D_{\mathrm{Ge}} \cdot \left( \frac{\partial^2 c_{\mathrm{Ge}}(r,t)}{\partial r^2} + \frac{1}{r}\frac{\partial c_{\mathrm{Ge}}(r,t)}{\partial r} \right) \tag{2}$$

which can be solved using a Green's function method [2], as follows:

$$c_{\mathrm{Ge}}(r,t) = \int_0^\infty \frac{c_{\mathrm{Ge}}(r,0)}{4\pi D_{\mathrm{Ge}} t} \cdot I_0\left(\frac{rr'}{2D_{\mathrm{Ge}}t}\right) \cdot \exp\left(\frac{-r^2 - r'^2}{4tD_{\mathrm{Ge}}}\right) \cdot 2\pi r' \cdot dr' \tag{3}$$

where $I_0$ is the modified Bessel function of the first kind.

Since the diffusion length is typically much smaller than the fiber diameter, the boundary impacts can be neglected. The interdiffusion along the $z$-axis is also negligible since the concentration gradient is much more gradual along the $z$-axis (given the typical temperature profiles of heating zones) than that along the $r$-axis. This is true everywhere but the region within $\pm(D_{\mathrm{Ge}} \cdot t)^{1/2}$ of the joint; optical simulation shows that some interdiffusion within this small region does not result in any significant difference in the light field.

A 3-D BPM method is needed for simulating fiber splices. A circular symmetry can be assumed to simplify the numerical scheme, if the loss from any misalignment is insignificant as compared with that from model-field mismatch. In a cylindrical coordination system $(z, r, \phi)$, the scalar Helmholtz (wave) equation is given by

$$\frac{\partial^2 E}{\partial z^2} + \frac{\partial^2 E}{\partial r^2} + \frac{1}{r}\frac{\partial E}{\partial r} + k_0^2 n^2(r,z) E = 0 \tag{4}$$

where $\lambda$ is the wavelength, $k_0 = 2\pi/\lambda$, and $n(r,z)$ is the RIP of the optical fiber splice, which vary (continuously) along the $z$-axis (beam propagation) in the vicinity of a fusion splice. $E(r,\phi,z) \cdot \exp(j\omega t)$ is a component of the electric field. $E(r,\phi,z)$ can be conveniently expressed as

$$E(r,\phi,z) = \varphi(r,z) \cdot \exp(-jk_0 n_0 z) \cdot \exp(jl\phi). \tag{5}$$

Here, $n_0$ is a reference refractive index. In the angular phase term, $l$ can be set to be zero for simulating splices between two single-mode fibers since a symmetrical $\mathrm{LP}_{01}$ is always launched from one end, and modes of $l \geq 1$ will not be excited. Applying the Páde (1, 1) approximation for wide-angle beam propagation [12], [13], an optical beam propagation equation is obtained, i.e.,

$$\frac{\partial \varphi}{\partial z} = \frac{-\frac{j}{2k_0 n_0}\left\{\frac{\partial^2}{\partial r^2} + \frac{1}{r}\frac{\partial}{\partial r} + k_0^2\left[n^2(r,z) - n_0^2\right]\right\}}{1 + \frac{1}{4k_0^2 n_0^2}\left\{\frac{\partial^2}{\partial r^2} + \frac{1}{r}\frac{\partial}{\partial r} + k_0^2\left[n^2(r,z) - n_0^2\right]\right\}}\varphi. \tag{6}$$

Yamauchi *et al.* deduced a finite-difference BPM algorithm using the Crank–Nicholson scheme [14], [15], where they define

$$\varphi(r,z) = \varphi\left((i-1)\cdot\Delta r, k\cdot\Delta z\right) = \varphi_{i,k} \tag{7}$$

and derived a set of linear equations to solve $\{\varphi_{i,k+1}\}_{i=1,2,\ldots,n+1}$ from $\{\varphi_{i,k}\}_{i=1,2,\ldots,n+1}$ and the RIPs [i.e., a beam propagation along the $z$-axis $(k \cdot \Delta z)$], as follows:

$$\begin{aligned}(2i-3)\cdot\varphi_{i-1,k+1} &+ (2i-2)\cdot\left[\beta+\Delta r^2 k_0^2\left(n_{i,k+1}^2 - n_0^2\right) - 2\right] \\ &\cdot \varphi_{i,k+1} + (2i-1)\cdot\varphi_{i+1,k+1} \\ &= (2i-3)\cdot\xi\cdot\varphi_{i-1,k} + (2i-2)\cdot\left\{\beta+\xi\cdot\left[\Delta r^2 k_0^2\left(n_{i,k}^2 - n_0^2\right) - 2\right]\right\} \\ &\cdot \varphi_{i,k} + (2i-1)\cdot\xi\cdot\varphi_{i+1,k}\end{aligned} \tag{8}$$

for $i > 1$, where the following constants are defined for convenience:

$$\begin{cases}\beta \equiv \frac{4k_0^2 n_0^2 \Delta r^2}{1+jk_0 n_0 \Delta z} \\ \xi \equiv \frac{1-jk_0 n_0 \Delta z}{1+jk_0 n_0 \Delta z}\end{cases}. \tag{9}$$

The corresponding equation at the origin ($r = 0$ or $i = 1$) was estimated by the L'Hospital's rule, as follows:

$$\begin{aligned}&\left[\beta+\Delta r^2 k_0^2\left(n_{1,k+1}^2 - n_0^2\right) - 4\right]\cdot\varphi_{1,k+1} + 4\varphi_{2,k+1} \\ &= \left\{\beta+\xi\cdot\left[\Delta r^2 k_0^2\left(n_{1,k}^2 - n_0^2\right) - 4\right]\right\}\cdot\varphi_{1,k} + 4\xi\cdot\varphi_{2,k}.\end{aligned} \tag{10}$$

Equations (8) and (10) are a set of tridiagonal linear equations, which can efficiently be solved by the Thomas algorithm $(O(n))$. In this paper, this algorithm is combined with diffusion simulation (3) to model the optical characteristics of fusion splices.

In this paper, MATLAB codes for solving the diffusion equation in fusion splices using the Green's function method and for implementing BPM using the Yamauchi algorithm [14], [15] have been developed. RIPs are calculated based on the concentration profiles. Light fields in the vicinity of the splices are simulated using the BPM code based on simulated RIPs from material diffusion simulations. Transparent boundary conditions are used because the reflection at the interfaces between silica glass and polymer coatings is typically negligible. The input field is set to be the fundamental $\mathrm{LP}_{01}$ mode of the launching fiber. The field is propagated through the splice (diffusion zone), and then, the corresponding $\mathrm{LP}_{01}$ mode of the receiving fiber is extracted by an overlap integral technique [2].

The diffusion simulation code is first tested and validated with various analytical solutions. The BPM code is first tested by calculating the following: 1) the far-field light power density of a Gaussian beam propagating in free space; 2) the $\mathrm{LP}_{01}$ modes; and 3) the butt–joint splice losses. The BPM results agree well with analytical solutions. To further validate the simulation scheme and codes, splice losses are simulated based on the measured RIPs and then compared with the measured splice losses. For three long-arc fusion splices, the measured splice losses are 0.20, 0.17, and 0.13 dB, respectively, whereas the simulated losses are 0.15, 0.11, and 0.09 dB, respectively. The measured losses are slightly greater than the simulated values, which can be well explained by the fact that misalignments between two fibers result in additional losses that are not modeled by the current circularly symmetrical scheme. Nonetheless, a clear correlation is evident, and the agreement between measured and simulated results is rather satisfactory.

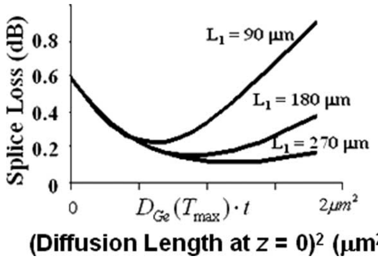


Fig. 2. Representative simulated splice loss versus $D_{\mathrm{Ge}}(T_{\max}) \cdot t$. $L_0 = 200\ \mu$m.

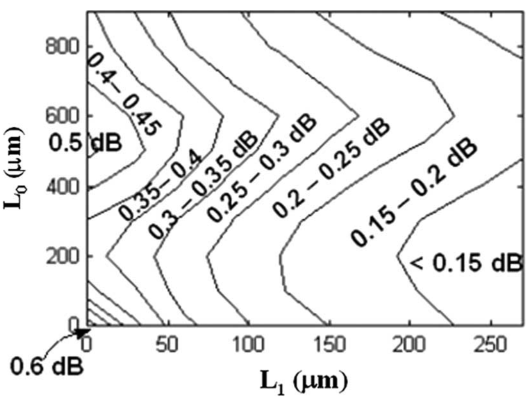


Fig. 3. Contour plot of the minimum splice loss (obtained at individual optimal $D_{\mathrm{Ge}}(T_{\max}) \cdot t$) in the space of the two key geometrical parameters of the heat zone: $L_0$ and $L_1$.

## III. Results and Discussions

Diffusion and BPM simulations have been conducted for 1000 splices at the wavelength of 1550 nm, in which ten levels are chosen for each of the three parameters, namely $L_0$, $L_1$, and $D_{\mathrm{Ge}}(T_{\max}) \cdot t$. The computation time for the diffusion and BPM simulation on a personal computer is less than 30 s per splice. Representative loss versus $D_{\mathrm{Ge}}(T_{\max}) \cdot t = L_{\mathrm{diff}}^2$, where $L_{\mathrm{diff}}$ is the "diffusion length" at the joint $z = 0$, is shown in Fig. 2. The unit for $D_{\mathrm{Ge}}(T_{\max}) \cdot t$ is micrometers. This parameter is used because of the diffusion scaling law, which states that an increase in diffusion time is equivalent to an increase in temperature as long as the resulting $D(T) \cdot t$ is kept the same. The splice loss decreases with increasing diffusion. For a set of fixed heat-source geometrical parameters $L_0$ and $L_1$, a minimum loss is always observed at an optimal $D_{\mathrm{Ge}}(T_{\max}) \cdot t$ (Fig. 2), beyond which, the splice loss increases again. The increase of the splice loss for prolonged diffusion is explained from the increased gradient in RIPs along the $z$-axis so that the modal conversion is less adiabatic, i.e., generating more radiation modes. This mechanism is verified by examining the simulated light fields. This conclusion is also consistent with the fact that the loss versus $D_{\mathrm{Ge}}(T_{\max}) \cdot t$ exhibits lower and shallower minima for more gradual heat sources (Fig. 2).

The achievable minimum losses for different $L_0$ and $L_1$ (with individual optimal $D_{\mathrm{Ge}}(T_{\max}) \cdot t$) are then shown in Fig. 3. The total width of the heat zone $(L_0 + 2L_1)$ is estimated to be 50–1000 $\mu$m for most of the commercial arc fusion splicers (and typically $> 2000\ \mu$m if a pre or post heat treatment is involved) based on the measured RIPs. Representative simulated RIPs and light intensities in the vicinity of the splices are

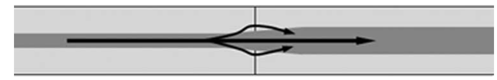

Fig. 4. Schematic illustration of the interference effect among the fundamental mode and radiation modes that results in the oscillation in Fig. 3.

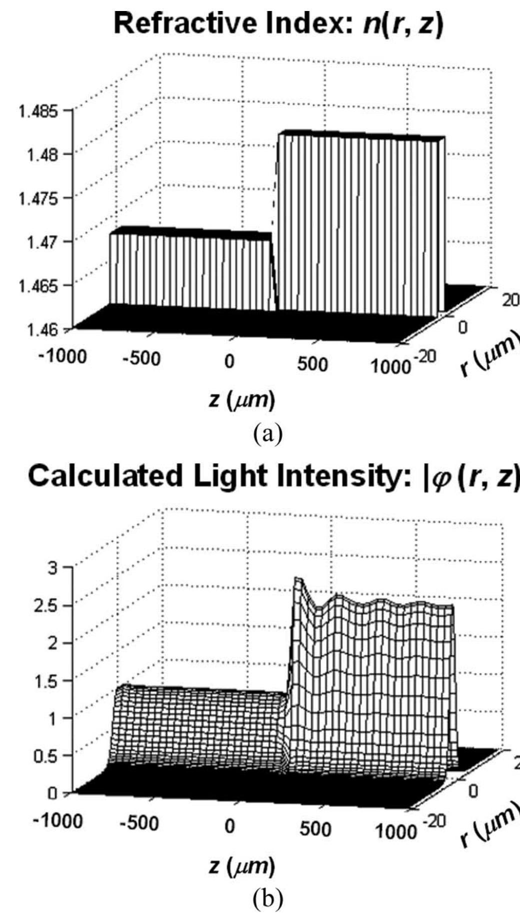


Fig. 5. (a) RIP and (b) calculated light intensity field for a butt–joint splice.

shown in Figs. 5 and 6. As shown in Fig. 3, a gradual transition temperature zone (large $L_1$) is essential for reducing loss. Furthermore, an interesting feature seen in Fig. 3 is the oscillation in "loss versus $L_0$" for a fixed $L_1$. This oscillation results from the modal interference between $\mathrm{LP}_{01}$ and higher order radiation modes in the diffusion zone. This modal interference effect is schematically illustrated in Fig. 4. Since the length of splices is small, modal noise is not expected to be significant. Thus, such recoupling can be beneficial for reducing loss. As $L_1$ increases, the mode conversion becomes gradual, and the modal interference decreases. This observation also clearly illustrates that the assumption of adiabatic mode conversion is not always (typically) correct for realistic fusion-splicing situations.

A similar modal interference effect can be seen in Fig. 5(b) for a butt–joint splice (i.e., the oscillation in the light intensity in the receiving fiber). In the case of a butt–joint splice, all radiation modes will eventually completely attenuate, and an observable oscillation in the simulated light field is typically an indication of a significant splice loss. On the other hand, in fusion splices with substantial diffusion, some of the light

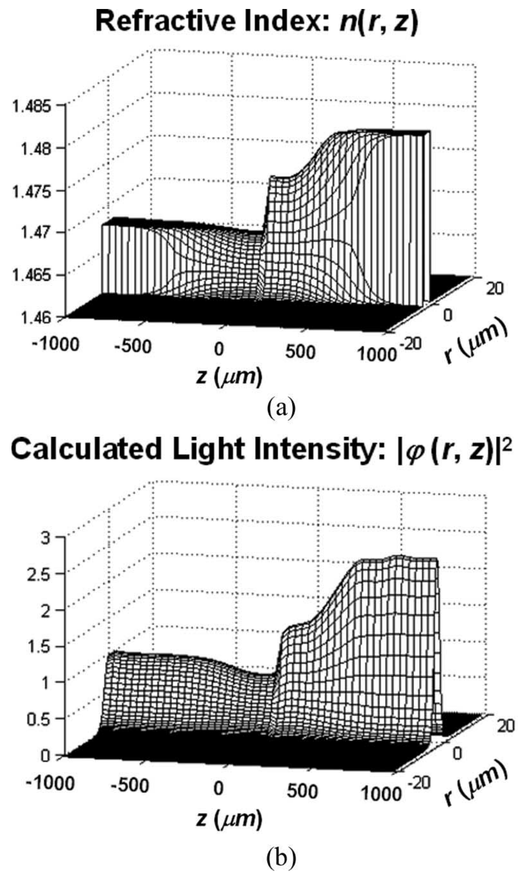


Fig. 6. Example of (a) calculated RIP (from diffusion simulation) and (b) associated simulated light intensity field for a diffused splice.

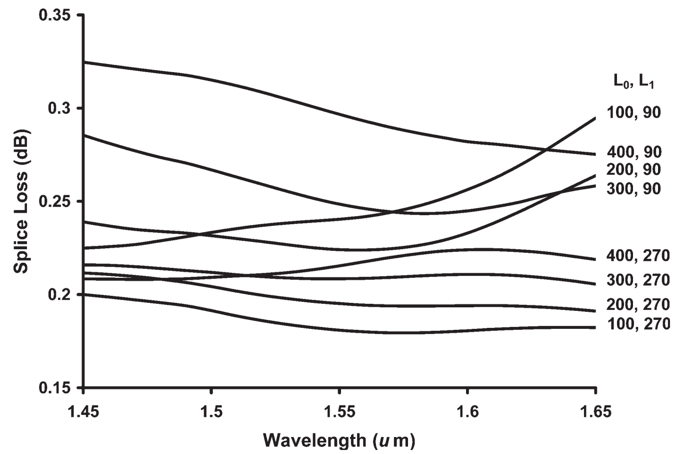


Fig. 7. Example of calculated wavelength-dependent splice losses with different geometrical parameters of the heat zone. The unit for $L_0$ and $L_1$ is micrometers. In this particular case, the splice loss increases with increasing $L_0$ because of an adverse interference effect.

in radiation modes can be recoupled into the $LP_{01}$ mode, and such an effect can be intentionally utilized to reduce splice loss between dissimilar fibers. In this case, oscillation in the light field is typically not observable [Fig. 6(b)], but the interference effect is indicated by an oscillation in splice loss versus a geometrical parameter of the heat zone (e.g., Fig. 3).

Wavelength-dependent splice losses can also be calculated (where wavelength-dependent $LP_{01}$ modes should be used). An example is given in Fig. 7. Although splice loss generally exhibits a weak dependence on the light wavelength, the wavelength dependence can be systematically changed from positive to negative values by tuning the geometry parameters of the heat zone. In principle, this phenomenon can be exploited for making wavelength-dependent attenuators if a precise control of the temperature profile can be achieved (which is technologically challenging but not impossible).

Knowing the general existence of nonadiabatic modal conversion in fusion splices, the requirement of an optimal amount of diffusion [represented by an optimal $D(T) \cdot t$, which can be alternatively adjusted by changing either the temperature or diffusion time] for minimizing the splice loss at any given geometrical profile of the heat zone and the (useful) optical interference effect provide insight for knowledge-based optimization of the fusion-splicing process and the design of new heat treatment devices/procedures to reduce dissimilar fiber splice losses.

The modeling scheme can be easily extended to the cases where more than one dopant is involved (e.g., when splicing DCF or EDF), where the diffusivities of each of the dopants must be known, and (uncoupled) diffusion equations should be independently solved.

While BPM is often the choice for the numerical analysis of beam propagation, alternatives exist. In particular, Marcuse has applied the coupled-mode theory (CMT) to model beam propagation through fiber tapers and demonstrated analogous interference phenomena [16].

Although this paper concerns reducing dissimilar fiber splice loss via dopant diffusion, there are other approaches for reducing splice loss. In particular, intermediate or bridge fibers can be used to reduce the splice loss between dissimilar fibers, and an optimal solution for selecting the intermediate fiber has recently been derived [17].

The same diffusion and BPM modeling methods and codes may be used for multimode fiber splices under the condition that the light field has a circular symmetry. Typically, the launching modes are no longer the $LP_{01}$ modes, and $l$ in (5) can be nonzero. Splice loss mechanisms for multimode fiber splices can be different.

These observed diffusion-related loss mechanisms for circularly symmetric cases should also occur in asymmetric fiber splices, e.g., for splices involving microstructured or polarization-maintaining fibers, where an asymmetrical 3-D simulation scheme can be further proposed.

## IV. Concluding Remark

Combining material diffusion and optical beam propagation simulations provides a powerful tool for understanding the loss mechanisms for dissimilar fiber splices with substantial diffusion. This paper shows that an optimal amount of diffusion is generally required to achieve the minimum splice loss for a given geometrical profile of the fusion/heating zone. Additional annealing beyond the optimal level is in fact detrimental because it makes the modal conversion less adiabatic. It should be noted that the modal conversion is generally not adiabatic with the optimal amount of diffusion since some light in the radiation modes in the transition region can be recoupled back to the fundamental mode, which reduces the loss. In fact, oscillation of splice loss with the geometrical parameters of the heating zone due to a modal interference effect is revealed, which can be intentionally used to reduce dissimilar fiber splice losses. In general, gradual transitions are critical to ensure a low splice loss and to reduce the interference effect.

The understanding of these loss mechanisms, along with the development of a combined material diffusion and optical BPM scheme for simulating splice losses (free open-source MATLAB codes are provided for downloading), is important for designing new fusion splicers and special heat treatment devices to reduce dissimilar fiber splice losses via diffusion and enables knowledge-based splicing process optimization.

## ACKNOWLEDGMENT

The author would like to thank Lucent Technologies, Inc., and OFS Fitel. This paper has significantly benefited from the author's prior splicing development work at Lucent and OFS (2001–2003). This paper is about general splicing loss mechanisms and modeling methods and does not include a specific work that is related to proprietary OFS products. Free, generic, and open-source MATLAB codes for material diffusion and optical BPM simulations of splice losses have been made available as part of the author's National Science Foundation CAREER project (DMR-0448879) education and outreach activities. They can be obtained by downloading at http://alum.mit.edu/www/jluo/OpenSourceCodes/ or by emailing the author.

## REFERENCES

[1] M. Nakano, H. C. Chandan, J. Luo, L. R. Pritchett, T. Ellithi, T. Veng, A. D. Yablon, and J. F. Ryan, "Improvements in splicing dissimilar fibers," in *Proc. 51st Int. Wire Cable Symp.*, 2001, pp. 687–695.

[2] A. D. Yablon, *Optical Fiber Fusion Splicing*. Berlin, Germany: Springer-Verlag, 2005.

[3] D. B. Mortimore and J. V. Wright, "Low-loss joints between dissimilar fibres by tapering fusion splices," *Electron. Lett.*, vol. 22, no. 6, pp. 318–319, Mar. 1986.

[4] J. T. Krause, W. A. Reed, and K. L. Walker, "Splice loss of single-mode fiber as related to fusion time, temperature, and index profile alteration," *J. Lightw. Technol.*, vol. LT-4, no. 7, pp. 837–840, Jul. 1986.

[5] H. Y. Tam, "Simple fusion splicing technique for reducing splicing loss between standard singlemode fibers and erbium-doped fiber," *Electron. Lett.*, vol. 27, no. 17, pp. 1597–1599, Aug. 1991.

[6] W. Zell, J. A. Becker, P. K. Bachmann, and W. G. Hermann, "Low-loss fusion splicing of PCVD-DFSM fibers," *J. Lightw. Technol.*, vol. LT-5, no. 9, pp. 1192–1195, Sep. 1987.

[7] W. X. Zheng, O. Hulten, and R. Rylander, "Erbium-doped fiber splicing and splice loss estimation," *J. Lightw. Technol.*, vol. 12, no. 3, pp. 430–435, Mar. 1994.

[8] T. Veng and B. Palsdottir, *Erbium-Doped Fiber Design for Improved Splicing Performance*, Part 1 ed. vol. 5623. Bellingham, WA: SPIE, 2004, pp. 438–446.

[9] S. Pradhan, J. Arbulich, and K. Srihari, *Splice Loss Optimization of Single Mode Fiber and Erbium Doped Fiber-Experiments and Issues*, vol. 3. Washington, DC: Amer. Soc. Mech. Eng., 2003, pp. 479–486.

[10] Q. Yu, P. H. Zongo, and P. Facq, "Refractive-index profile influences on mode-coupling effects at optical-fiber splices and connectors," *J. Lightw. Technol.*, vol. 11, no. 8, pp. 1270–1273, Aug. 1993.

[11] G. Kweon and I. Park, "Splicing losses between dissimilar optical waveguides," *J. Lightw. Technol.*, vol. 17, no. 4, pp. 690–703, Apr. 1999.

[12] Y. Ohtera, O. Hanaizumi, and S. Kawakami, "Numerical analysis of eigenmodes and splice losses of thermally diffused expanded core fibers," *J. Lightw. Technol.*, vol. 17, no. 12, pp. 2675–2682, Dec. 1999.

[13] B. Zamzow, G. Ruegenberg, M. Anderson, and W. Knop, "Numerical simulation of high quality fiber optic splices for high precision loss evaluation," in *Proc. Int. Wire Cable Symp.*, 1999, pp. 621–628.

[14] J. Yamauchi, Y. Akimoto, M. Nibe, and H. Nakano, "Wide-angle propagating beam analysis for circularly symmetric waveguides: Comparison between FD-BPM and FD-TDM," *IEEE Photon. Technol. Lett.*, vol. 8, no. 2, pp. 236–238, Feb. 1996.

[15] J. Yamauchi, K. Nishio, and K. Nakano, "Analysis of a lensed coreless fiber by a hybrid technique combining FD-BPM and FD-TDM," *J. Lightw. Technol.*, vol. 16, no. 3, pp. 465–471, Mar. 1998.

[16] D. Marcuse, "Mode conversion in optical fibers with monotonically increasing core radius," *J. Lightw. Technol.*, vol. LT-5, no. 1, pp. 125–133, Jan. 1987.

[17] A. D. Yablon and M. Sumetsky, "Optimum intermediate fibers for reducing interconnection loss: Exact solution," *Opt. Lett.*, vol. 32, no. 6, pp. 617–619, Mar. 15, 2007.

**Jian Luo** received the B.E. degrees in materials science and engineering and in electronics and computer technology from Tsinghua University, Beijing, China, in 1994 and the M.S. degree in materials science and engineering and the Ph.D. degree in ceramics from Massachusetts Institute of Technology, Cambridge, in 1999 and 2001, respectively.

After receiving the Ph.D. degree, he worked in industry for more than two years with Lucent Technologies, Inc., and OFS Fitel/Furukawa Electric Co., Norcross, GA. In August 2003, joined the School of Materials Science and Engineering, Clemson University, Clemson, SC, as an Assistant Professor. He is also affiliated with the Center for Optical Materials Science and Engineering Technologies, Clemson University. In 2005, he enjoyed a one-month summer faculty research appointment with Oak Ridge National Laboratory, Oak Ridge, TN.

Prof. Luo was the recipient of the Ralph E. Powe Junior Faculty Enhancement Award in 2005, the National Science Foundation CAREER Award in 2005, and the Air Force Office of Scientific Research Young Investigator Award in 2007.